Paleomagnetic Secular Variation and Environmental Magnetism of Holocene-aged Sediments from Tulare Lake, CA

By

Janine Marie Roza

A Thesis Submitted to the Department of Geological Sciences

California State University Bakersfield

In Partial Fulfillment for the Degree of Masters of Science in Geology

Spring 2015

Paleomagnetic Secular Variation and Environmental Magnetism of Holocene-aged Sediments from Tulare Lake, CA

By

Janine Marie Roza

This thesis or project has been accepted on behalf of the Department of Geological Sciences by their supervisory committee:

Rob Negrini
Committee Chair

Dirk Baron

Daniel McCuan

Abstract

The lake-level record from Tulare Lake, CA has been shown to provide valuable constraints on late Pleistocene and Holocene channelized runoff from the Sierra Nevada mountain range into the San Joaquin Valley of California, one of the world's most prolific agricultural centers. This project focuses on the use of magnetic properties of the Tulare Lake sediments in order to test previous results by dating the sediments and determining the relative lake level at the time of deposition. Toward this end, sediments exposed by a trench dug in the southeastern end of the Tulare Lake bed in the Poso Canal were sampled for magnetic analyses. Shallowing lake conditions were identified leading up to a prominent unconformity from magnetic mineralogy and grain size indicators, primarily decreasing ARM/IRM and S-Ratio values suggesting coarser grain sizes and more oxidizing conditions. Approximately half of the samples possessed well-behaved paleomagnetic directions suitable for paleomagnetic secular variation dating. The results indicate that the sediments below the unconformity were deposited approximately 7600-6700 ^{14}C years ago (~7600 to 8500 cal yr B.P.), and the sediments above the unconformity were deposited approximately 2200-500 ^{14}C years ago. The ages of the corresponding sediments are consistent with the time intervals during which lake level was predicted to be above the elevation of the Poso Canal site before and after a mid-Holocene regression.

1. Introduction

The Tulare Lake bed is located in the southern San Joaquin Valley, in Kings County California (Figure 1). Its central coordinates are 36.00 °N, 119.72 °W and it covers

approximately 1600 square kilometers. Currently dry due to agriculture diversion, Tulare Lake was the largest fresh water lake west of the Great Lakes with respect to area, with depths reaching up to 12 meters [Preston, 1981]. The Kings, Kaweah, Tule, and Kern Rivers feed the Tulare Lake basin from the Sierra Nevada and discharge from these rivers controls Tulare Lake-levels as shown by hydrologic balance models [Atwater et al., 1986]. Tulare lake-level is therefore controlled by climate-driven changes in the Sierran precipitation and runoff. This hypothesis is further supported by the consistency of this lake-level history over the past 10,000 years with other paleo-lake records from south-central California [Bacon et al., 2006; Negrini et al., 2006; Kirby et al., 2012]. The purpose of this project was to test previous lake-level records obtained from exposures and core from the western edge of the lake by studying the magnetic properties of the Tulare Lake sediments from the south-east side of this large lake basin. The paleomagnetic secular variation (PSV) method [e.g., Bradley, 1999] was used to date these new exposures toward testing their predicted ages above and below an unconformity that represents a middle Holocene lowstand of the lake, predicted by previous work. In addition, magnetic properties of sediments were investigated to determine the composition, concentration, and grain-size of magnetic minerals, which are used as proxies for lake conditions, flood events and regional climate change [Evans and Heller, 2003].

2. Previous Work

Building upon earlier works by Davis [1999] and Atwater et al. [1986], Negrini et al. [2006] used stratigraphy and radiocarbon dating primarily from trench exposures on the west side of the lake basin (Figure 1) to constrain several major fluctuations in Tulare Lake level throughout the Holocene. Blunt [2013] elaborated on this by constraining the lake level in the

north-western part of Tulare Lake using geochemical and geophysical data and primarily with clay percent, where higher clay percent corresponds to deeper lake conditions. Both of the above studies identified a middle Holocene lowstand wherein the lake surface rarely, if ever, reached an elevation higher than 61-62 masl from ~7500 to 3000 cal yr B.P. At the other end of the basin at a slightly higher elevation (63-64 masl), Jackson et al. [2014] used lithologic descriptions and radiocarbon dating from an exposure dug into the side of the Poso Canal to help constrain lake level. Radiocarbon dating was problematic, as there was significant variation in the dates returned from the bulk sediment, gastropod shells, anodonta shells, and charcoal, which was likely due to a varying reservoir effect in the lake [Philippsen, 2013]. Though the radiocarbon dating was problematic, the most reliable ages (from charcoal) in Jackson et al. [2014] revealed an unconformity (Figure 2) associated with absence of deposition during the middle Holocene lowstand identified by the previous studies. The unconformity lies within a coarse-grained unit with abundant shell fragments. It separates units consisting of lacustrine silts and clays. There is also no evidence supporting any large scale deformation, such as slumps or folds [Jackson et al., 2014]. The purpose of the present study is to better constrain the age of the lowstand represented by the unconformity by comparing a PSV record from the sediments below and above the unconformity with a previously published, well dated PSV record from the western U.S., the Fish Lake, Oregon record [Verosub et al., 1987] (Figure 2). The PSV ages correspond to the predicted dates from the highest lake levels shown by Blunt [2013] and Blunt and Negrini [in press] with clay percent. The previous work is summarized in Figure 2.

3. Methods

This project focuses on sediments from a trench that was dug in the southern Tulare lake bed in the Poso Canal (Figure 2). The Poso Canal site is approximately 63-64 masl [Jackson et al. 2014] and is in a sub-basin of the lake separated from its main body by a sand spit (Figure 1). The total stratigraphic depth sampled in the trench was approximately four meters. On top of the sampled section were two meters of road-fill. Samples were taken continuously at two-centimeter spacing, and oriented in the field using a Brunton compass. Magnetizations of these samples were measured at the UC Davis Paleomagnetics Laboratory and the Institute for Rock Magnetism laboratories in Minnesota to determine environmental magnetic properties and paleomagnetic vector components. At UC Davis, discrete samples were measured in their original plastic containers using 2G Enterprises 755-1.65UC DC SQUID Superconducting Rock Magnetometer. The natural remanent magnetization (NRM) was measured after alternating field demagnetization (AFD) at steps of 0,5,10,15,20,25,30,35,40,50,60,80 and 100 mT. Anhysteretic remanent magnetization (ARM) and isothermal remanent magnetization (IRM) were also measured after the same set of demagnetization steps. S-ratio measurements of 100 mT and -30 mT were also done at UC Davis. At the Institute for Rock Magnetism laboratories, a set of samples was crushed and put into small capsules or beakers to be analyzed. These samples are representative of depths throughout the studied interval. A Princeton Measurements vibrating sample magnetometer was used to measure the magnetic saturation (M_S), the saturation remanence (M_r), the coercivity (H_C), and the coercivity of remanence (H_{Cr}). A KappaBridge susceptibility meter was used to determine the temperature dependent susceptibility. Susceptibilities were measured at different frequencies with a MAGNON variable frequency susceptibility meter, which was used for identifying superparamagnetic grains. A Quantum

Designs magnetic properties measurement system (MPMS) measured magnetization *vs* temperature with varying magnetic fields; this was used for magnetic mineral identification.

4. Sediment Magnetization

4.1 Demagnetization of NRM

Approximately half of the samples possessed well-behaved paleomagnetic directions, as defined by stable, single-component magnetizations, indicated by linear decay to the origin of orthogonal magnetization components over a range of AFD treatments when plotted on a Zijderveld diagram [Zijderveld, 1967] (Figure 3). There is commonly a viscous magnetic overprint [Tauxe et al., 2010], which is demagnetized by 10 mT AFD.

4.2 Paleomagnetism and Rock Magnetism *vs* Depth

The paleomagnetic and rock magnetic data *vs* depth are summarized in Figure 4. The declination and inclination are shown for the sections where rock magnetic and demagnetization properties indicate stable directions. The NRM, IRM, ARM, susceptibility and NRM/ARM all show significantly increased values leading up to the unconformity, while the ARM/IRM and S-Ratio show significantly decreasing values leading up to the unconformity.

4.3 Other Rock Magnetism

The temperature vs magnetization results from the MPMS were consistent throughout the measured interval and a representative sample is shown (Figure 5). The presence of magnetite is indicated, by the 120 K transition, which corresponds to the Verwey transition temperature of magnetite [Özdemir and Dunlop, 1993] and goethite, by the negative slope on the room

temperature (RT) remanence curves [Bilardello and Jackson, 2013]. The uncorrected hysteresis loops had a steep positive slope indicating a strong paramagnetic component, which is likely due to the high volume of clays in the sediment [Sandgren and Snowball, 2001, Tauxe et al. 2010]. The corrected loop shows the magnetic contribution of all ferrimagnetic grains (Figure 6). There was no apparent variation of the loops throughout the interval, and a representative sample is shown. The tightness of the loops supports pseudo-single domain grain size, while loop closure under ± 200 mT supports a magnetite mineralogy [Tauxe et al., 2010]. Figure 7 is a Day plot with the boundaries from Day et al. [1977] shown. While all of the samples fall within the pseudo-single domain boundaries, this is typical of natural samples [Tauxe et al., 2010], but there is a trend between decreasing M_r/M_s values and decreasing stability of the NRM. The samples from below the unconformity generally have the highest M_r/M_s values and show the most stable NRM, while the samples for this study that fell below 0.1 M_r/M_s had unstable NRM and were not able to be successfully used for PSV correlation. None of the samples that were measured showed any susceptibilities that were frequency dependent, which indicated the absence of any superparamagnetic grains. The temperature-dependent susceptibility data (Figure 8), shows a distinct change in behavior at approximately 3m depth, which corresponds to the unconformity; for samples below the unconformity the cooling curves mirror the heating curves, while for samples above the unconformity the cooling curve has increased values compared to the heating curve, and this increase starts at approximately 580 degrees Celsius, which is the Curie temperature for magnetite [Dunlop and Özdemir, 1997]. This suggests that above the unconformity a new mineral is present that converts to magnetite upon heating. However, Minyuk et al. [2013] show this could also be caused by the presence of arsenic in the sediments

beneath the unconformity but not directly above, since arsenic suppresses the formation of magnetite [Minyuk et al., 2013].

5. Environmental Magnetism Implications

Magnetic grain size increases upsection, which is inferred from decreasing ARM/IRM values [Evans and Heller, 2003] (Figure 9), and corresponds to periods of lake shallowing, as coarser grains are generally deposited in shallower water [Boggs, 2006]. Larger percentages of hematite, which is recognized by lower S-ratio values, also could correspond to lower lake levels, since magnetite is more likely to oxidize to hematite in shallower, more oxidized water [Evans and Heller, 2003]. The stratigraphy does not show evidence of an influx of soil-derived particles into the lake sediments, nor that extensive soil development had occurred on the lake sediments themselves, and this is supported by the fact that none of the samples showed frequency-dependent susceptibilities, which are characteristic of superparamagnetic grains [Evans and Heller, 2003].

6. Paleomagnetic Secular Variation Dating

Sediments from Poso Canal demonstrated stable, single-component vector data, and therefore the inclination and declination are compared with a reference record for western North America [Lund, 1996], specifically Fish Lake Oregon [Verosub et al., 1986]. The Fish Lake record was chosen for comparison because of its proximal location, approximately 900 km north of Tulare Lake (Figure 1). Relative paleointensity was not used for correlation because the samples from this study do not show uniform grain sizes or mineralogy (Figure 4), both of which are needed for reliable intensity correlations [Tauxe et al., 2010]. There are stable directions in

two sections: one section occurs in Unit 1 and the other section occurs in Unit 4 (Figure 2). The sediments from above the unconformity had exaggerated amplitudes, and therefore a Gaussian smoothing function was applied to facilitate correlation. The results indicate that the sediments below the unconformity were deposited approximately 7600-6700 ^{14}C years ago (~7600 to 8500 cal yr B.P.), and the sediments above the unconformity were deposited approximately 2200-500 ^{14}C years ago. (Figure 10).

7. Conclusion

This project set out to date the Tulare Lake sediments in order to test the interpretation of a middle Holocene unconformity and its predicted age (Negrini et al., 2006; Jackson et al., 2014; Blunt and Negrini, in press), and was successful in doing so. The sediments above were predicted to be no younger than 7500 cal yr B.P. and the sediment above, no older than ~3000 cal yr B.P. The finding of this study demonstrated that the sediments below were deposited approximately from ~7600 to 8500 cal yr B.P., and the sediments above the unconformity were deposited approximately 2200-500 cal yr B.P.. This project was also able to recognize shallowing lake conditions leading up to an unconformity from magnetic mineralogy and grain size indicators, primarily decreasing ARM/IRM and S-Ratio values.

Acknowledgements. This research has been fully supported by the CSUB Center for Research Excellence in Science and Technology, which is funded by the National Science Foundation (NSF EHR #1137774). This project also benefitted from a fellowship granted to the principal author by the Institute for Rock Magnetism in Minnesota, as well as grants from the CSUB Graduate Student Center and Student Research Scholars Program. We thank Ken Verosub for

use of his lab. Land access permission was granted by John and Joe Gebhardt of GFM, Wasco, CA and Mazal Orchards, LLC. We thank Eric Heaton, Brandon Jackson and Logan Prosser for their help in the field and Jihadda Govan of the Bureau of Land Management for fruitful discussions leading to the identification of the Poso Canal site. We are grateful for comments on an early manuscript by D. McCuan. The data used for this study can be made available by contacting the primary author.

References

Atwater, B.F., D.P. Adam, J.P. Bradbury, R.M. Forester, R.K. Mark, W.L., Lettis, G.R. Fisher, K.W. Gobalet, and S.W. Robinson (1986), A Fan Dam for Tulare Lake, California, and implications for the Wisconsin Glacial history of the Sierra Nevada. Bulletin of the Geological Society of America 97, 97–109.

Bacon, S.N., R.M., Burke, S.K. Pezzopane, and A.S. Jayko (2006), Late glacial maximum and Holocene lake levels of Owens Lake, eastern California, USA. Quaternary Science Reviews.

Bilardello D. and M. Jackson (2013), What do the Mumpsies do? The IRM Quarterly Vol 23 No.3

Bradley, R.S. (1999), Paleoclimatology, Academic Press, San Diego, 610pp

Blunt, A. (2013), Latest Pleistocene through Holocene Lake Levels from the TL05-4 Cores, Tulare Lake, CA. M.S. Thesis, Department of Geological Sciences, California State University, Bakersfield, CA.

Blunt, A., and R.M. Negrini (In Press). Latest Pleistocene through Holocene Lake Levels from the TL05-4 Cores, Tulare Lake, CA. Quaternary International

Boggs, S. J. (2006), Principles of Sedimentology and Stratigraphy: Fourth Edition, Upper Saddle River, New Jersey, Prentice Hall.

Cohen, A.S. (2003), Paleolimnology, Oxford, 499 p

Davis, O.K. (1999), Pollen analysis of Tulare Lake, California: great basin-like vegetation in central California during the full-glacial and early Holocene. Review of Palaeobotany and Palynology 107, 249–257.

Day, R., M. Fuller, and V. A. Schmidt (1977), Hysteresis properties of Titanomagnetites: Grain size and composition dependence, Phys. Earth Planet. Inter., 13, 260–267

Dunlop, D. J., and Ö. Özdemir (1997), Rock Magnetism. Fundamentals and Frontiers. Cambridge Studies in Magnetism Series. Cambridge University Press

Evans, M.E., and F. Heller (2003), Environmental Magnetism, Academic Press, 299 p

Jackson, B., L. Prosser, K. Padilla, and L. Medina (2014), Holocene-Aged Lake Sediments of the Southeastern Margin of Tulare Lake CA, Paper presented at PSAAPG, Bakersfield CA.

Kirby, M.E., S.R.H. Zimmerman, W.P. Patterson, and J.J. Rivera (2012), A 9170-year record of decadal-to-multi-centennial scale pluvial episodes from the coastal Southwest United States: a role for atmospheric rivers? Quaternary Science Reviews 46, 57-65.

Lund, S.P., (1996), A Comparison of Holocene Paleomagnetic Secular Variation Records from North America, Journal of Geophysical Research, Vol 101 p 8007-8024

Minyuk, P. S., T. V. Subbotnikova, L. L. Brown, and K. J. Murdockm (2012), High-temperature thermomagnetic properties of vivianite nodules, Lake El'gygytgyn, Northeast Russia. Clim. Past, 9, 433–446

Negrini, R.M., P.E. Wigand, S. Draucker, K. Gobalet, J.K. Gardner, M.Q. Sutton, and R.M. Yohe II. (2006), The Rambla Highstand Shoreline and the Holocene lake level history of Tulare Lake, California. Quat.Sci. Rev., 25: 1599-1618

Özdemir, Ö., and D.J. Dunlop (1993), Chemical remanent magnetization during γFeOOH phase transformations. Journal of Geophysical Research Vol 98, 0148-0227

Page, R.W. (1986), Geology of the fresh ground-water basin of the Central Valley, California, with texture maps and sections. US Geological Survey Professional Paper 1401C

Philippsen, B. (2013), The freshwater reservoir effect in radiocarbon dating. Heritage Science Volume 1, Number 1

Preston, W.L., (1981), Vanishing Landscapes: Land and Life in the Tulare Lake Basin. University of California Press, Berkeley, CA.

Sandgren, P., and I. Snowball (2001), Application of mineral magnetic techniques to Paleolimnology in ed. Last William M., Smol, John P., Birks Harry B. 2001. Tracking Environmental Change Using Lake Sediments: Volume 2: Physical and Geochemical Methods. Springer Science & Business Media, 504 p

Tauxe, L, S.K. Banerjee, R.F. Butler, and R. van der Voo (2010), Essentials of Paleomagnetism. UC Press 512p.

Verosub, K. L., P. J. Mehringer Jr., and P. Waterstraat (1986), Holocene secular variation in western North America: Paleomagnetic record from Fish Lake, Hamey County, Oregon, Journal of Geophysical Research, Vol 91, 3609- 3623.

Zijderveld, J.D.A. (1967), The natural remanent magnetization of the Exeter Volcanic Traps (Permian, Europe). Tectonophysics 4: 121-153.

Figure 1. Location of Tulare Lake and simplified geologic map modified from Page [1986]. The Poso Canal Site is located in the southeast part of the lake, and is marked by a star. The work from Blunt [2013] was conducted on core sediments from the northwest part of the lake; the coring site is shown as a diamond on the map. The location of the site corresponding to the Fish Lake paleomagnetic secular variation record is shown in the inset.

Figure 2. Previous work context. The Poso Canal outcrop photo is shown, along with the stratigraphic units characterized by Jackson et al. [2014]. The unconformity lies within a coarse-grained unit with abundant shell fragments. It separates units consisting of lacustrine silts and clays. The PSV record from Fish Lake [Verosub et al., 1986] is also shown. The age predicted for the oldest sediments above the unconformity and the youngest sediments below the unconformity are indicated, as well as the depths at which PSV dating was successful for this study. The PSV ages from the present study correspond to the predicted ages that were derived from the highest lake levels shown by the clay percent proxy in Blunt [2013]. The 45% clay line

plotted in the Figure is shown to indicate the depth above which there was predicted to be deposition at the Poso Canal site, as well as the corresponding time intervals.

Figure 3. Paleomagnetic demagnetization graphs. The Poso Canal samples from Units 1 and 4 (3a and 3c) demagnetize pseudo-exponentially and have single-component Zijderveld plots [Zijderveld, 1967] that show linear decay to the origin, behaviors which indicates stable magnetizations. The samples taken from elsewhere in the section (e.g., a sample from the unconformity layer shown here) do not possess those characteristics.

Figure 4. Magnetic data *vs* depth. The declination and inclination are shown for the sections where PSV correlation was successful for dating. The location of the unconformity is highlighted. The NRM, IRM, ARM, susceptibility and NRM/ARM all show significantly increased values leading up to the unconformity, while the ARM/IRM and S-Ratio show significantly decreasing values leading up to the unconformity. NRM/ARM, NRM/IRM, and NRM/k are not sufficiently consistent to allow for their use as relative paleointensity estimators.

Figure 5. Magnetization *vs* temperature. The 120 K transition, which corresponds to the Verwey transition temperature of magnetite [Özdemir and Dunlop, 1993], indicates significant magnetite within the samples, and the presence of goethite is indicated by the negative slope on the (RT) remanence curves [Bilardello and Jackson, 2013].

Figure 6. Hysteresis loop. The tightness of the loops supports pseudo-single domain grain size, while loop closure under ± 200 mT supports a magnetite mineralogy [Tauxe et al., 2010].

Figure 7. Day plot with boundaries from Day et al. [1977] shown. All of the samples fall within the pseudo-single domain boundaries, as is typical of natural samples [Tauxe et al., 2010]. The samples from Unit 1 are shown in oval A, while the samples from Unit 4 are shown in oval B. In addition, the samples for this study that fell below 0.1 M_r/M_s were not able to be successfully used for PSV correlation.

Figure 8. Temperature-dependent susceptibility graphs. The Poso Canal location shows two distinct behaviors, and representative samples from above and below the unconformity are shown; the cooling curves mirror the heating curves for samples below the unconformity, while for samples above the unconformity the cooling curve has increased values compared to the heating curve, and this increase starts at approximately 580 degrees Celsius, which is the Curie temperature for magnetite [Dunlop and Özdemir, 1997]. This suggests that magnetite was created in the heating of those samples.

Figure 9. ARM/IRM and S-Ratio vs Depth. The location of the unconformity is highlighted. For the ARM/IRM graph; lower values indicate larger grain size [Evans and Heller, 2003], which is interpreted as shallower lake conditions as the sediments approach the unconformity from below. For the S-Ratio graph; lower values indicate increasing hematite [Evans and Heller, 2003], which is likely due to oxidation from lower lake levels or exposure to the surface.

Figure 10. Paleomagnetic Secular Variation correlation. The data from this study is shown next to, and at the same declination and inclination scales as, the reference data [Verosub et al. 1986].

The zero degree line for declination and a line showing the expected geocentric axial dipole inclination for the two sites are shown. The data from above the unconformity is shown both as individual data points and as smoothed-fit lines. The results indicate that the sediments below the unconformity were deposited approximately 7600-6700 ^{14}C years (~7600 to 8500 cal yr B.P.) ago, and the sediments above the unconformity were deposited approximately 2200-500 ^{14}C years ago.

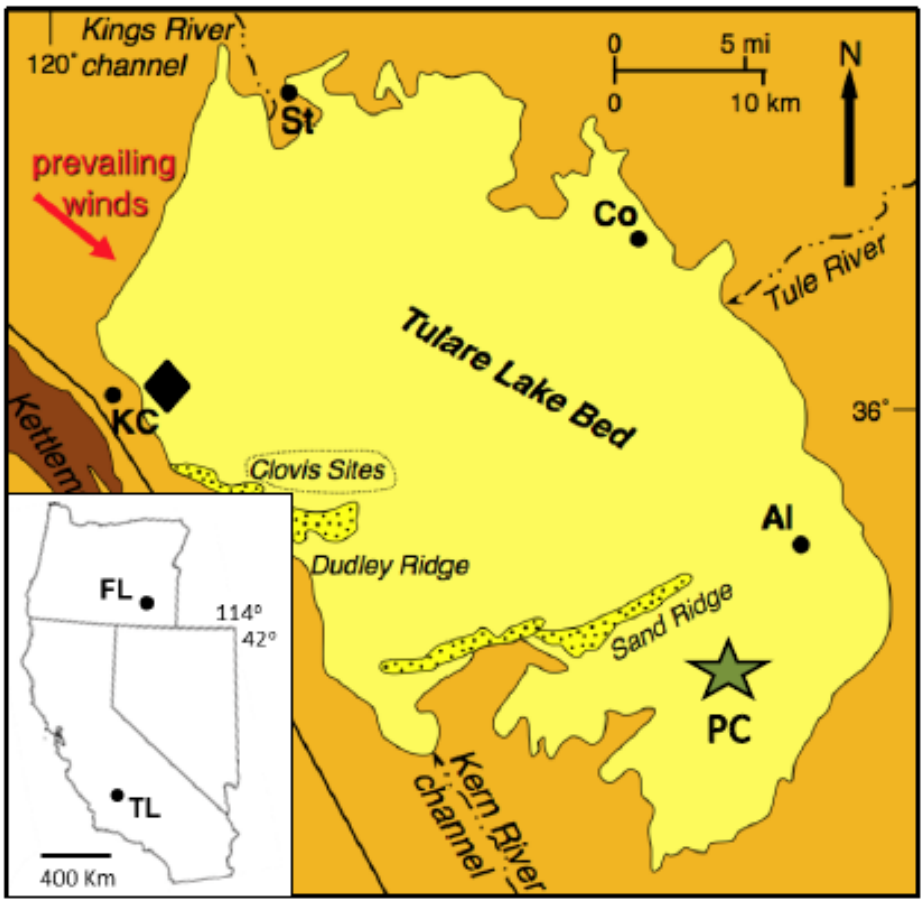
Kings River
120° channel
prevailing winds
St
0
5 mi
0
10 km
N
Co
Tule River
Tulare Lake Bed
KC
Kettlem
Clovis Sites
36°
Al
Dudley Ridge
Sand Ridge
PC
Kern River channel
FL
114°
42°
TL
400 Km

Figure 1

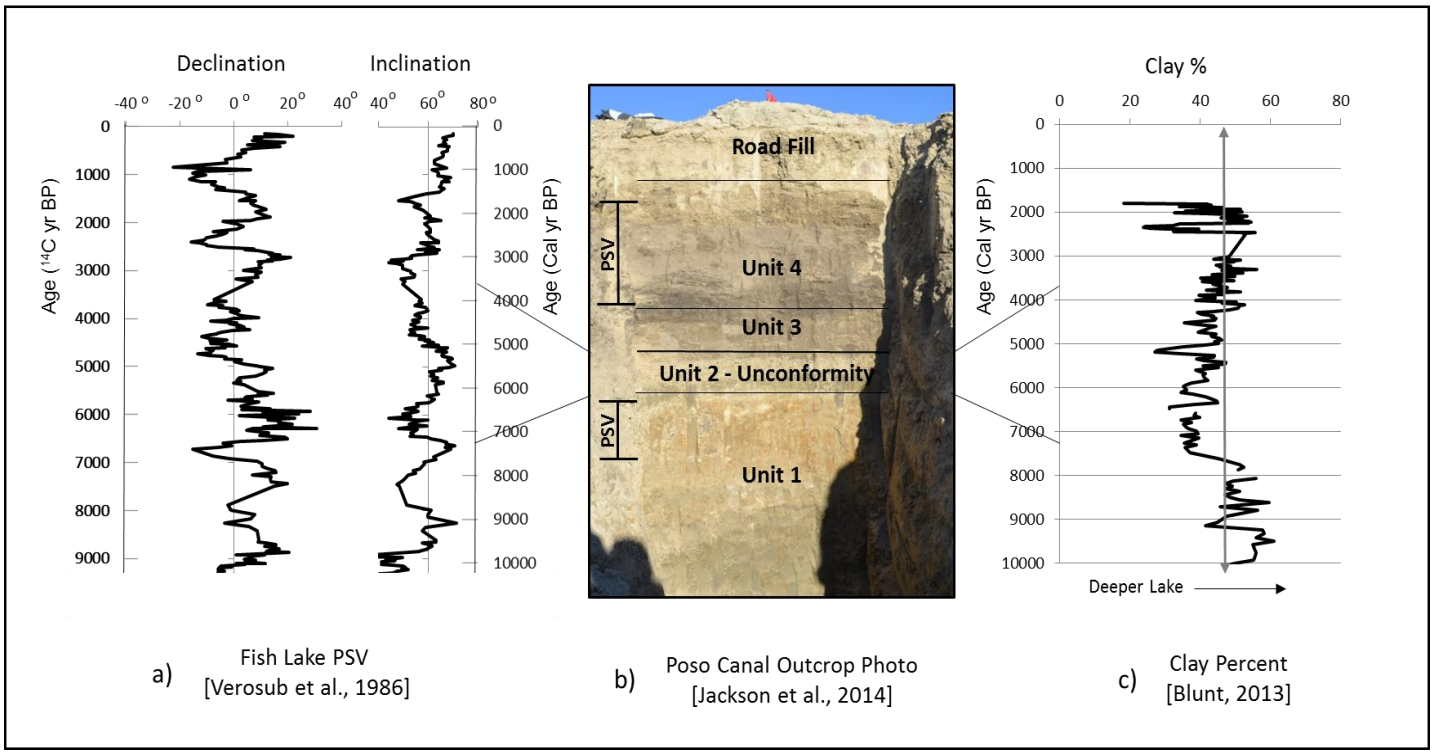
Declination
Inclination
Clay %
Age (^{14}C yr BP)
Age (Cal yr BP)
Road Fill
Unit 4
Unit 3
Unit 2 - Unconformity
Unit 1
PSV
PSV
Deeper Lake
a) Fish Lake PSV [Verosub et al., 1986]
b) Poso Canal Outcrop Photo [Jackson et al., 2014]
c) Clay Percent [Blunt, 2013]

Figure 2

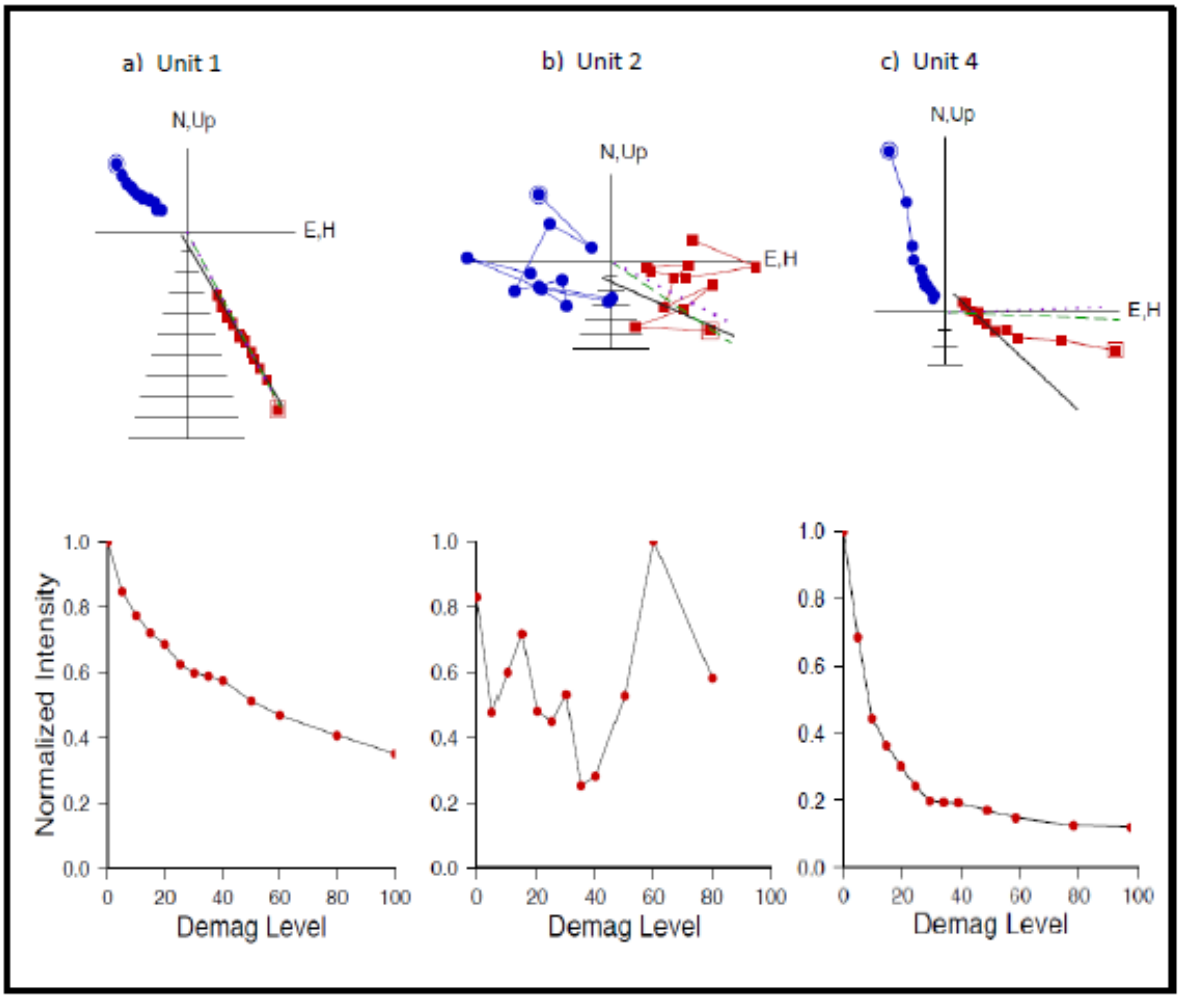
a) Unit 1
b) Unit 2
c) Unit 4
N,Up
E,H
Normalized Intensity
Demag Level
0.0
0.2
0.4
0.6
0.8
1.0
0
20
40
60
80
100

Figure 3

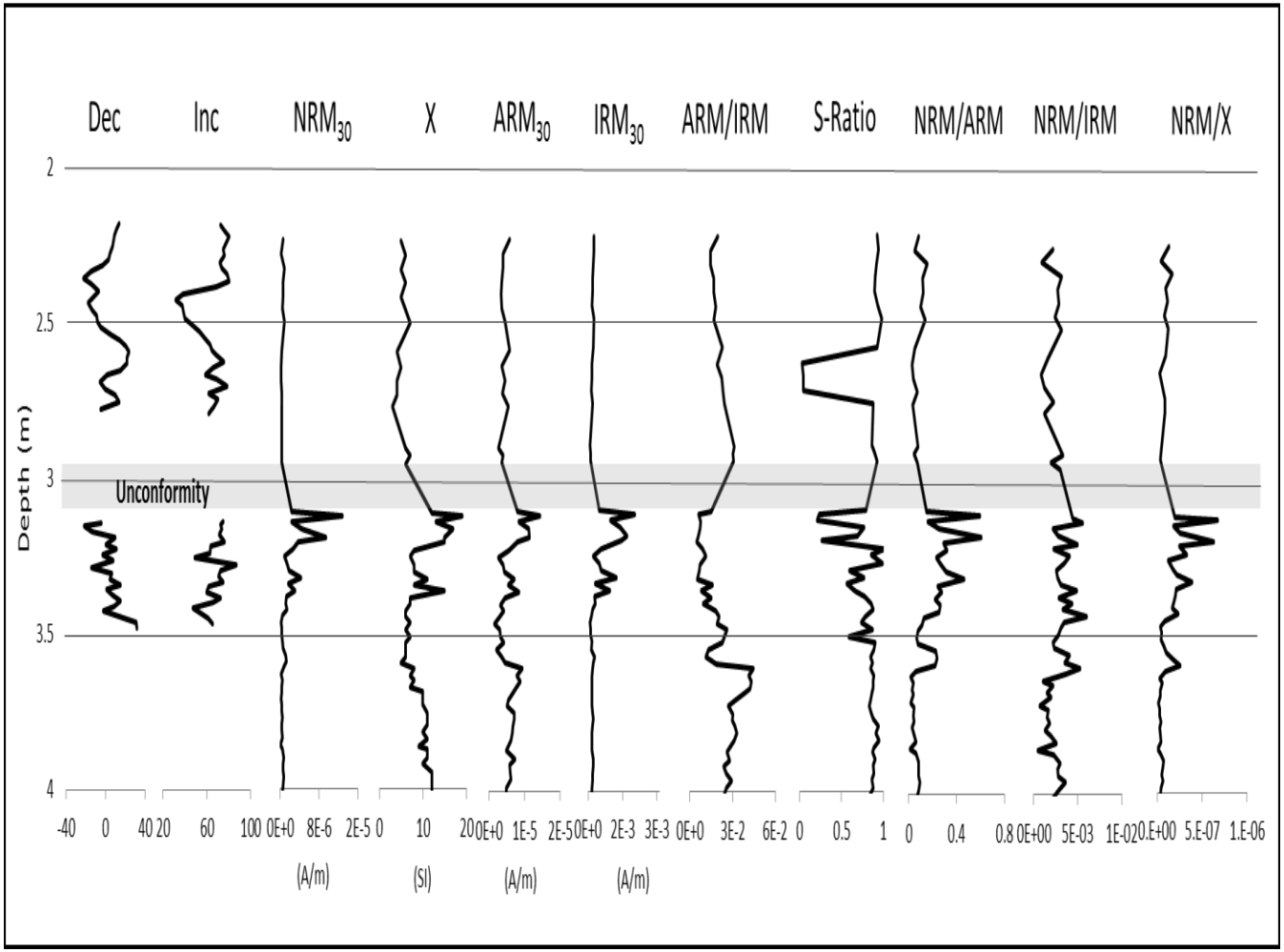
Dec
Inc
NRM30
X
ARM30
IRM30
ARM/IRM
S-Ratio
NRM/ARM
NRM/IRM
NRM/X
Depth (m)
2
2.5
3
3.5
4
Unconformity
-40 0 40
20 60 100
0E+0 8E-6 2E-5
(A/m)
0 10 20
(SI)
0E+0 1E-5 2E-5
(A/m)
0E+0 2E-3 3E-3
(A/m)
0E+0 3E-2 6E-2
0 0.5 1
0 0.4 0.8
0E+00 5E-03 1E-02
0.E+00 5.E-07 1.E-06

Figure 4

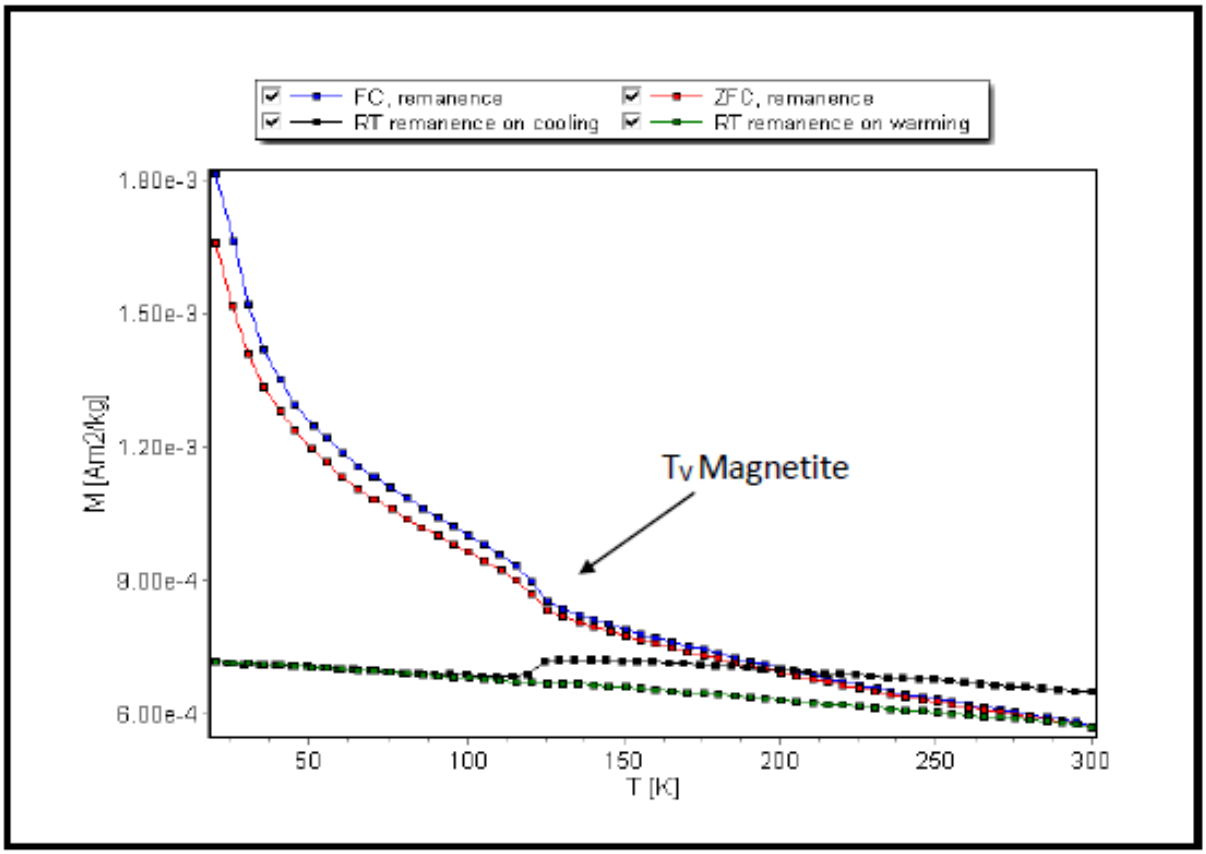
FC, remanence
ZFC, remanence
RT remanence on cooling
RT remanence on warming
1.80e-3
1.50e-3
1.20e-3
9.00e-4
6.00e-4
M [Am2/kg]
Tv Magnetite
50
100
150
200
250
300
T [K]

Figure 5

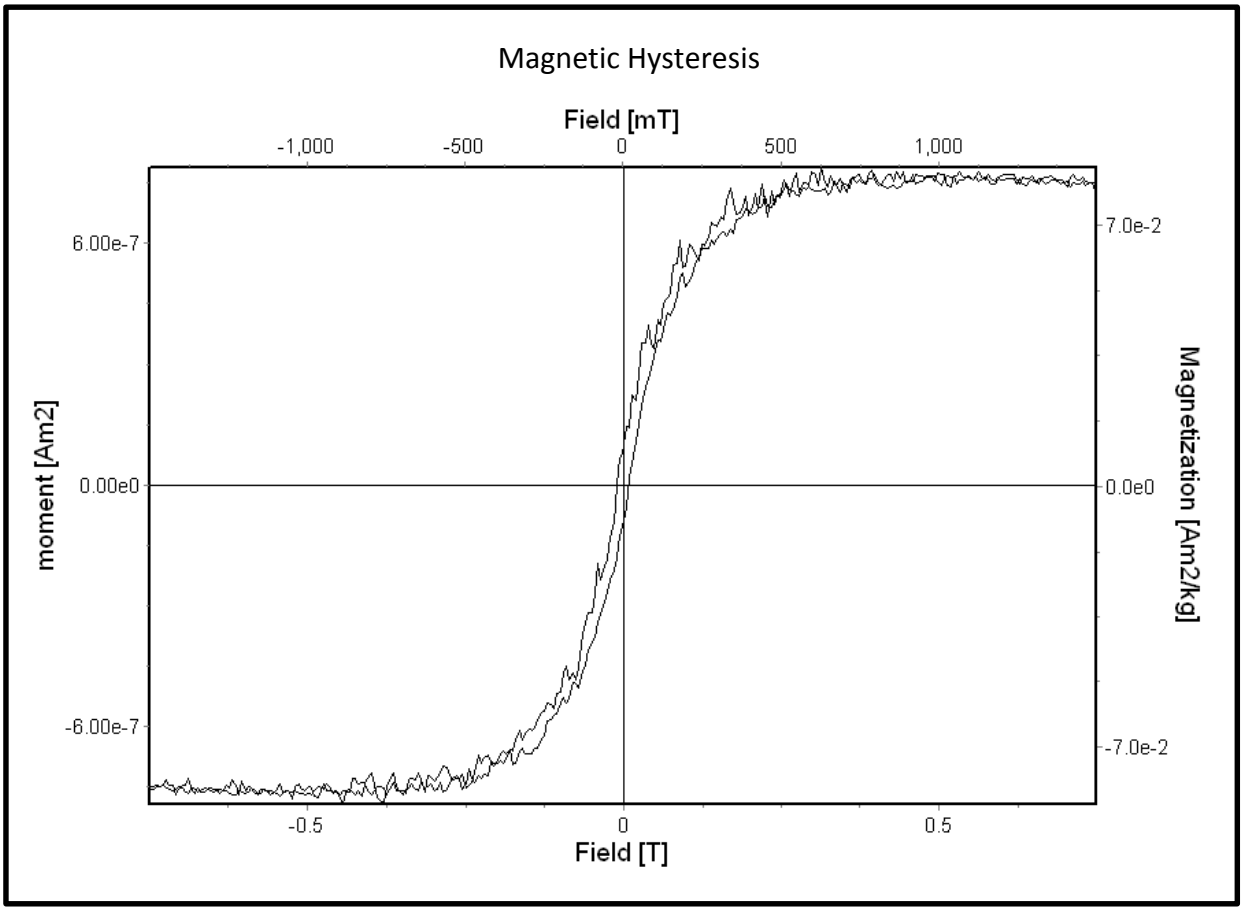
Magnetic Hysteresis
Field [mT]
-1,000
-500
0
500
1,000
6.00e-7
0.00e0
-6.00e-7
moment [Am2]
7.0e-2
0.0e0
-7.0e-2
Magnetization [Am2/kg]
-0.5
0
0.5
Field [T]

Figure 6

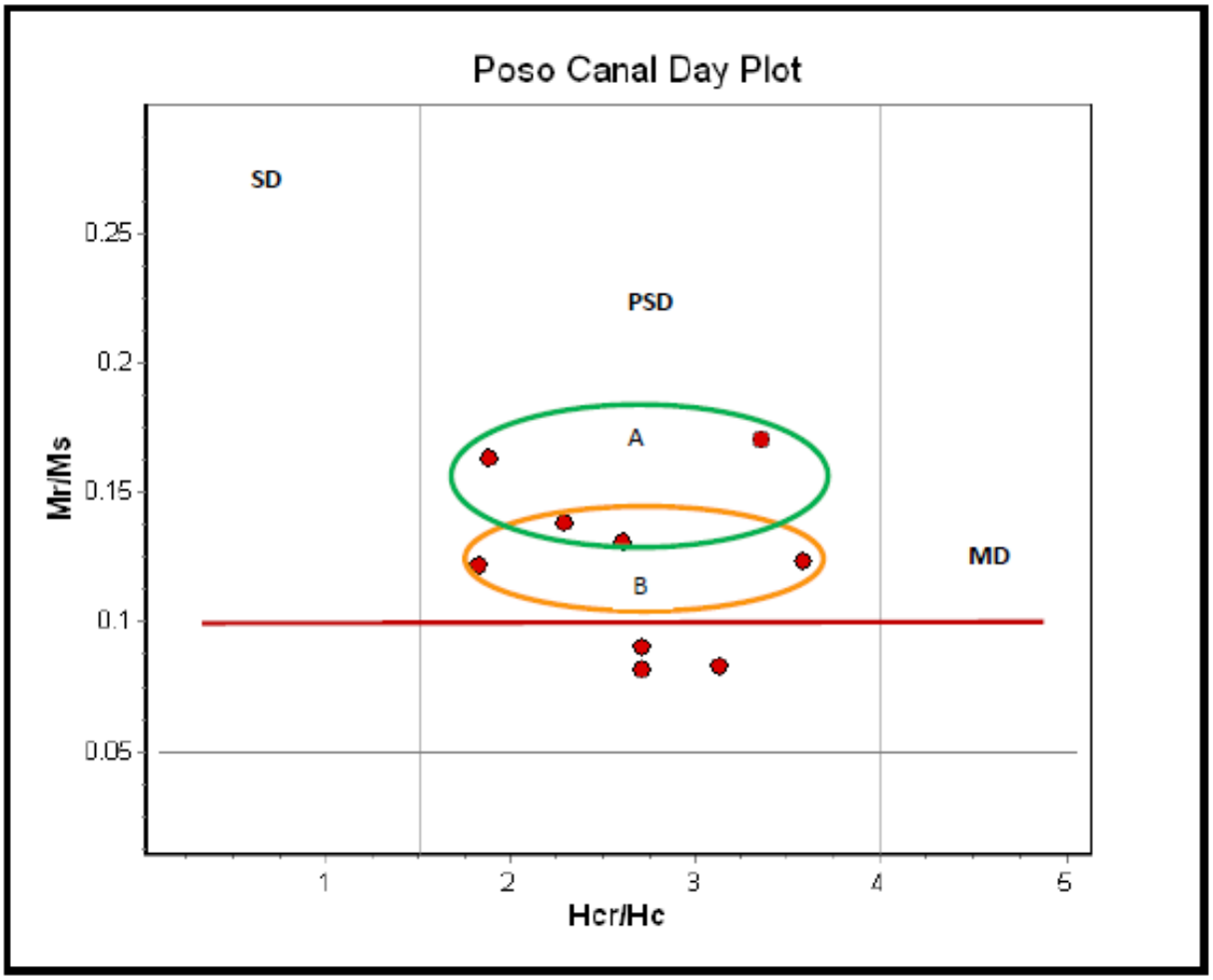
Poso Canal Day Plot
SD
PSD
MD
A
B
0.25
0.2
0.15
0.1
0.05
Mr/Ms
1
2
3
4
5
Hcr/Hc

Figure 7

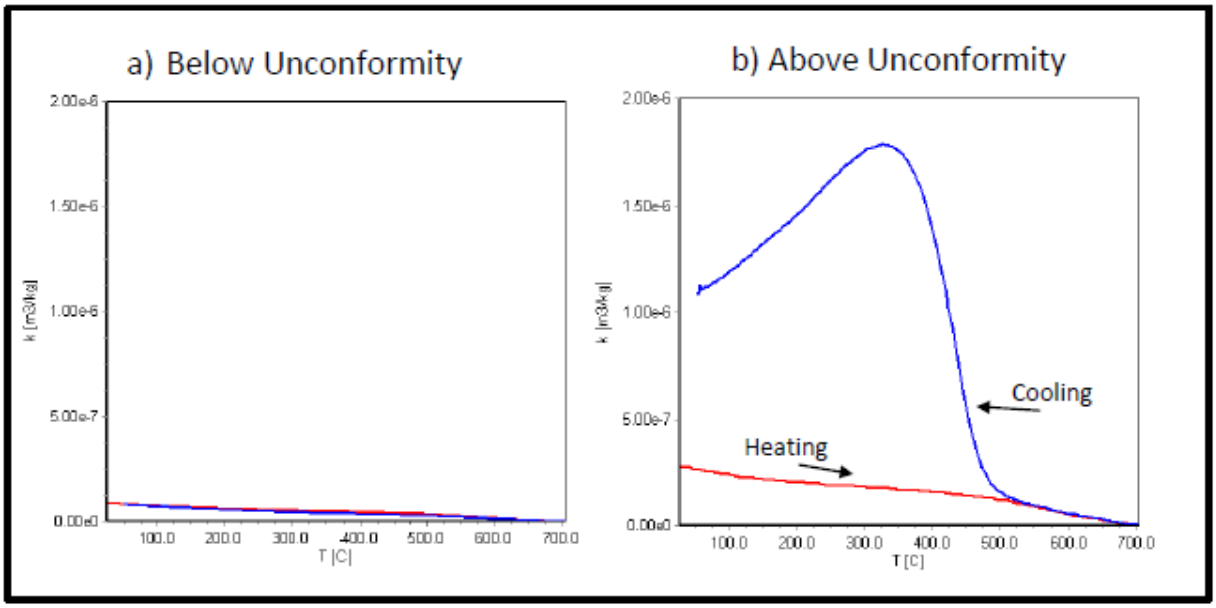
a) Below Unconformity
b) Above Unconformity
2.00e-6
1.50e-6
1.00e-6
5.00e-7
0.00e0
k [m3/kg]
100.0
200.0
300.0
400.0
500.0
600.0
700.0
T [C]
Cooling
Heating

Figure 8

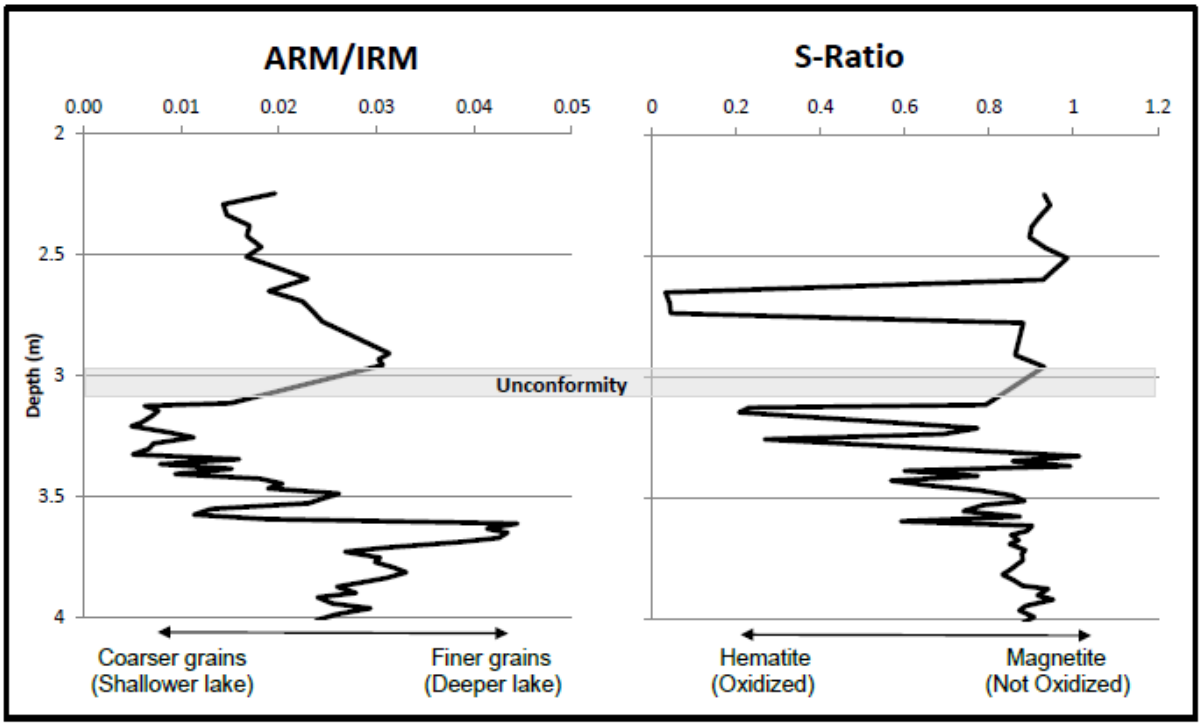

Figure 9

Figure 9

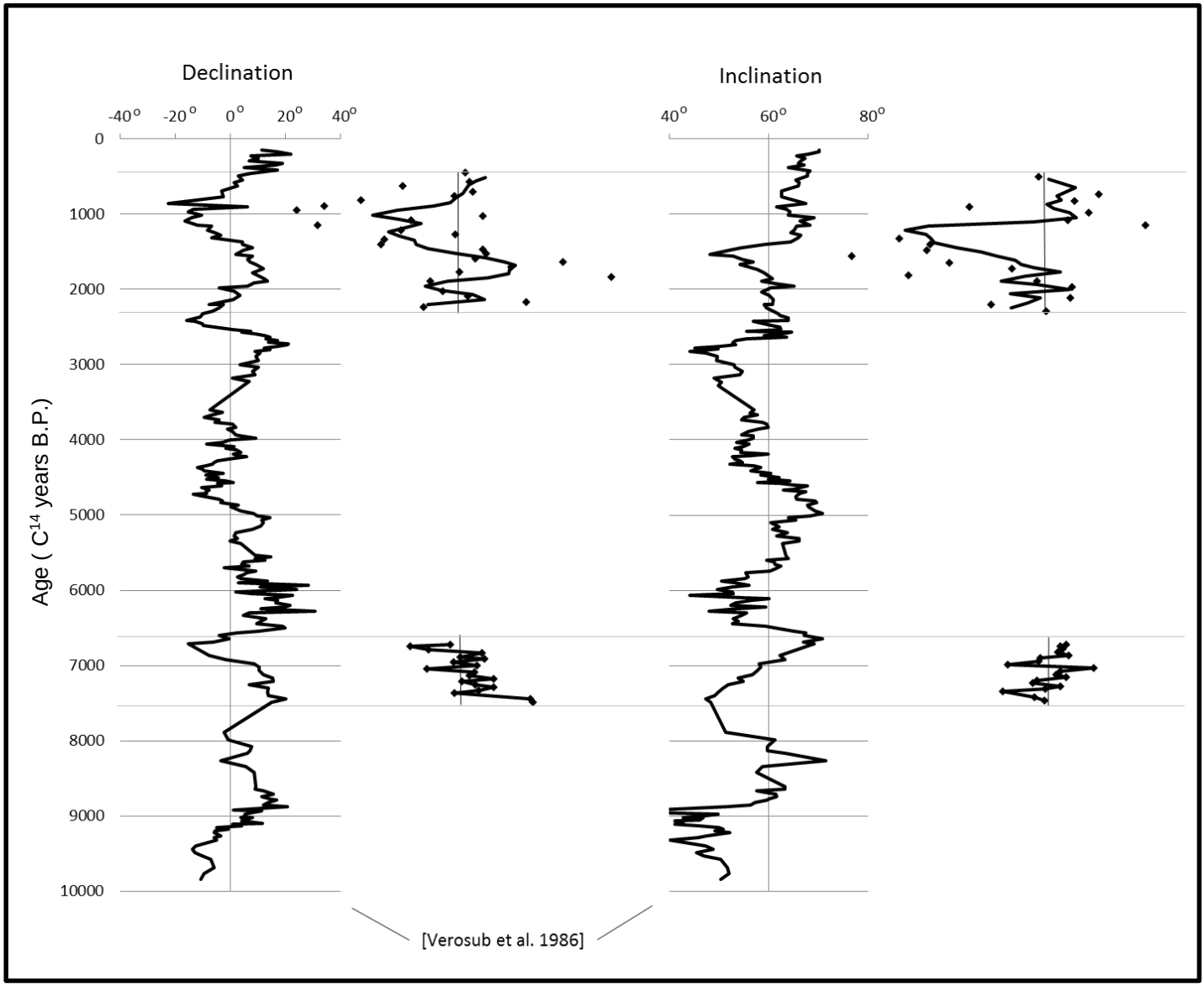
Declination
Inclination
-40°
-20°
0°
20°
40°
40°
60°
80°
0
1000
2000
3000
4000
5000
6000
7000
8000
9000
10000
Age (C14 years B.P.)
[Verosub et al. 1986]

Figure 10